

Article

Photosynthesis Traits of Pioneer Broadleaves Species from Tailing Dumps in Călimani Mountains (Eastern Carpathians)

Andrei Popa^{1,2} and Ionel Popa^{1,2,*} 

¹ Forestry Faculty, Ștefan cel Mare University of Suceava, Universității 13, 720229 Suceava, Romania; popa.andrei.dorna@gmail.com

² National Institute for Research and Development in Forestry Marin Drăcea, Calea Bucovinei 73bis, 725100 Câmpulung Moldovenesc, Romania

* Correspondence: popaicas@gmail.com; Tel.: +4-074-465-0967

Abstract: The reforestation and stable ecological restoration of tailings dumps resulting from surface mining activities in the Călimani Mountains represent an ongoing environmental challenge. To assess the suitability of different tree species for restoration efforts, photosynthetic traits were monitored in four broadleaf pioneer species—green alder (*Alnus alnobetula* (Ehrh.) K. Koch), aspen (*Populus tremula* L.), silver birch (*Betula pendula* Roth.), and goat willow (*Salix caprea* L.)—that naturally colonized the tailings dumps. Green alder and birch had the highest photosynthetic rate, followed by aspen and goat willow. Water use efficiency parameters (WUE and iWUE) were the highest for green alder and the lowest for birch, with intermediary values for aspen and goat willow. Green alder also exhibited the highest carboxylation efficiency, followed by birch. During the growing season, net assimilation and carboxylation efficiency exhibited a maximum in late July and a minimum in late June. The key limitation parameters of the photosynthetic process derived from the FvCB model (V_{cmax} and J_{max}) were the highest for green alder and exhibited a maximum in late July, regardless of the species. Based on photosynthetic traits, the green alder—a woody N₂-fixing shrub—is the most well-adapted and photosynthetically efficient species that naturally colonized the tailings dumps in the Călimani Mountains.

Keywords: gas exchange; ecosystem restoration; mountain forests; photosynthesis



Citation: Popa, A.; Popa, I. Photosynthesis Traits of Pioneer Broadleaves Species from Tailing Dumps in Călimani Mountains (Eastern Carpathians). *Forests* **2021**, *12*, 658. <https://doi.org/10.3390/f12060658>

Academic Editor: Francois Girard

Received: 12 May 2021
Accepted: 21 May 2021
Published: 22 May 2021

Publisher's Note: MDPI stays neutral with regard to jurisdictional claims in published maps and institutional affiliations.



Copyright: © 2021 by the authors. Licensee MDPI, Basel, Switzerland. This article is an open access article distributed under the terms and conditions of the Creative Commons Attribution (CC BY) license (<https://creativecommons.org/licenses/by/4.0/>).

1. Introduction

Climate change and anthropic activities have given rise to the most serious environmental problems of the 21st century [1]. Today, in an increasing number of ecosystems, anthropic influences are harming biodiversity and ecosystem functioning. Human activities change the condition of natural vegetation, leading to disturbances such as degradation of vegetation, erosion of soil, decline in land productivity and even reduction of ecosystem services [2].

A large proportion of the Earth's geological resources (metals, minerals, fuel, etc.) are underground; mining activities to access these resources damage the above-ground landscape and have a significant impact on natural ecosystems such as forests, rivers and lakes [3]. Even after the mining activity is complete (especially in the case of surface mining), dump areas remain in the place of former natural ecosystems and have the potential to cause serious environmental problems. Due to social and political pressure to undertake more sustainable development, the restoration of mining areas has gradually become an important phase of mining activities [4]. Multiple restoration solutions are available; of these, soil amendment combined with phytoremediation (reforestation) is the most environmentally friendly method [5].

Due to high soil degradation (lack of nutrients and organic matter, small edaphic volume, high concentration of heavy metals), it is important to choose a mix of species that are well-adapted to the local climate and the unique conditions of the mining habitat [6].

Successful reforestation of these degraded landscapes depends on the adaptability of tree species to degraded soil and the capacity of plant associations to contribute to the restoration of soil proprieties and former environmental conditions [7].

The process of ecosystem reconstruction on degraded mining soils progresses gradually from dump consolidation and soil amendments to pioneering species installation and finally climax tree species establishment [8]. In many cases, human interventions through ecological reconstruction are informed by the natural colonization of pioneer species. The optimal species composition for reforestation is chosen based on criteria such as adaptative capacity (survival rate), growth and biomass production (photosynthesis), and the capacity to cover the land through vegetative or generative regeneration [7].

In mountainous areas (e.g., the Carpathians), pioneer species colonize open soils on degraded or abandoned lands as part of primary succession. These pioneer species include green alder (*Alnus alnobetula* (Ehrh.) K. Koch = *Alnus viridis* (Chaix) DC), aspen (*Populus tremula* L.), silver birch (*Betula pendula* Roth.), goat willow (*Salix caprea* L.) and rowan (*Sorbus aucuparia* L.) [9]. Green alder, an N₂-fixing shrub, plays an important role in mountain ecosystems due to its capacity to stabilize slopes and prevent erosion [10,11]. On the other hand, silver birch is a fast-growing deciduous species that occurs naturally throughout most of Europe and is frequently observed on degraded lands [12,13]. Aspen and goat willow have high ecological amplitudes and are widely distributed throughout the temperate and boreal areas of Europe and Asia [14,15].

Carbon assimilation, as an indicator of species' adaptability to specific habitat conditions, is related to biomass production, CO₂ storage, competitiveness and survival capacity [16]. Gas exchange measurements play a major role in understanding photosynthetic processes [17,18]. The performance of forest species in terms of photosynthetic traits is evaluated through gas exchange, which is measured under controlled experimental conditions or in situ conditions [19,20]. Particular growing conditions specific to mining-degraded soils modify the normal assimilation process [21–23].

To the best of our knowledge, no previous studies have measured gas exchange to analyse the photosynthetic traits of mountain pioneer species growing in former mining areas. However, analyses of photosynthetic parameters under different growing conditions (exposure to ozone, fertilization variants, enriched CO₂, etc.) have been performed for *Populus* spp. [24–26], *Salix* spp. [27–29], *Betula* spp. [30–32], and *Alnus* spp. [33–35].

Our work aimed to quantify the eco-physiological performance of four broadleaf pioneer species that naturally colonized a mountain tailings dump area. The following scientific questions were examined: (i) Which of these four pioneer species is best adapted for use in reforestation processes from the point of view of photosynthetic traits? (ii) What are the seasonal patterns of the photosynthetic traits?

2. Materials and Methods

2.1. Study Site

This study took place in the Călimani Mountains (Eastern Carpathians, Romania; 47°7'24" N and 25°13'48" E; 1500 m a.s.l.) on degraded tailings dumps resulting from sulfur surface mining that occurred between 1969 and 1997. During this period, the former natural forest ecosystem (a mixture of Norway spruce and Swiss stone pine) and organic soil were destroyed, and dumps were formed by the successive storage of tailings. In 2007, an ecological reconstruction effort began with the stabilization of the slopes with high slants, alkaline amendment of the soil (debris from former buildings) and afforestation of some areas with Norway spruce (*Picea abies* L., H. Karst.) and green alder. Currently, the upper part of the mining dump is colonized by pioneer forest species (green alder, aspen, goat willow, birch) in combination with herbaceous species, and the area is characterized by a primary succession of vegetation [9,36].

The woody species present on the site comprise species specific to the upper mountain area: green alder, Norway spruce, dwarf mountain pine (*Pinus mugo* Turra), aspen, goat willow and birch. Shrubby vegetation is represented by blueberry (*Vaccinium myr-*

tillus L.), cranberry (*Vaccinium vitis-idaea* L.), bog blueberry (*Vaccinium uliginosum* L.) and rhododendron (*Rhododendron myrtifolium* Schott & Kotschy).

Air temperature (2 m) and soil water content (10 cm depth) were measured using dedicated sensors (HOBO U23-001, Onset Computer Corporation, Bourne, MA, USA and CS650, Campbell Scientific, Logan, UT, USA). The average annual air temperature at the site in 2019 was 4.3 °C and, in the vegetation season, it was 10.7 °C (Figure 1). The average annual precipitation in the study area is 1000–1200 mm. The snow layer is present for an average of 180–200 days each year, the first snowfall can occur in early October, and the typical vegetation season starts in the second decade of May until middle October [37].

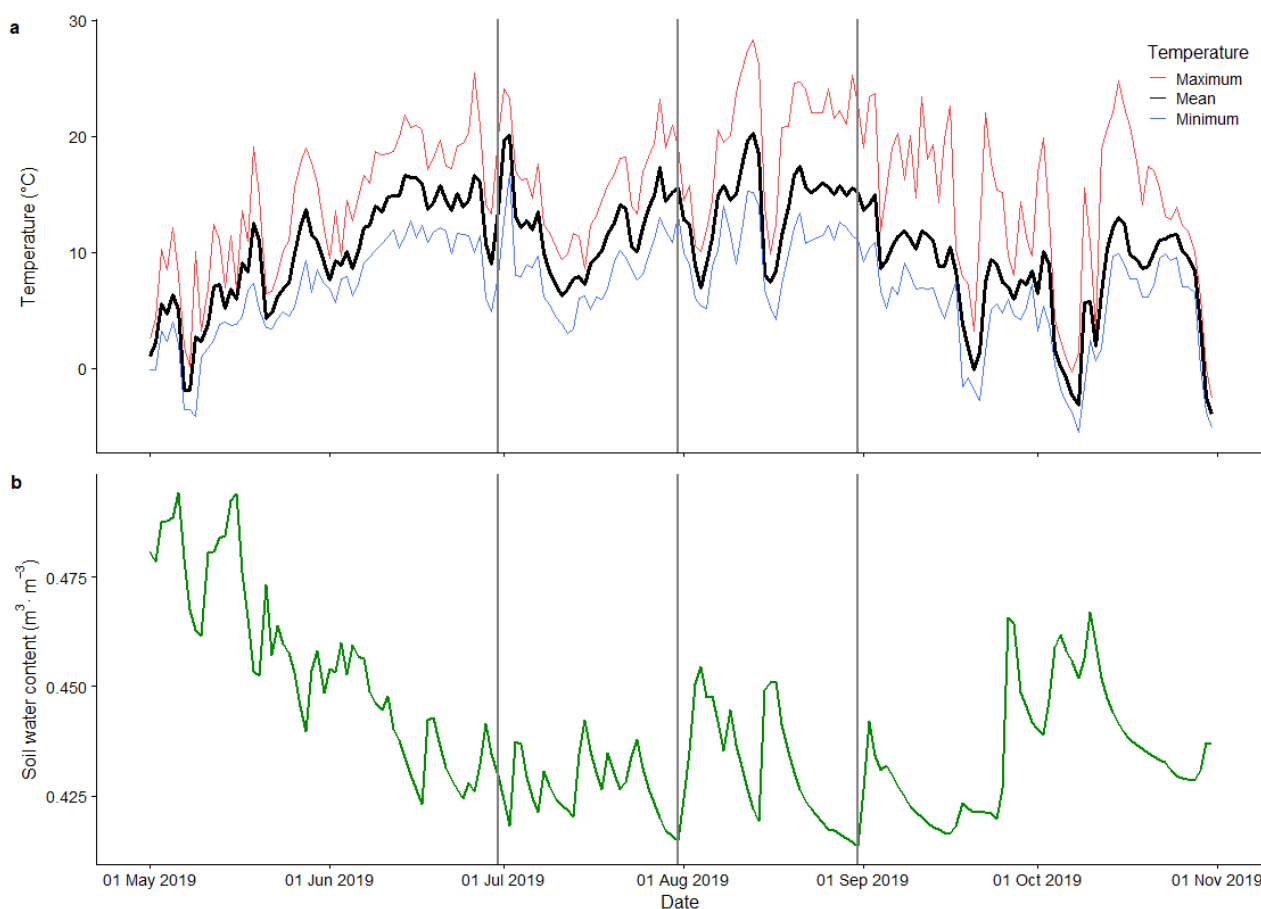


Figure 1. Air temperature (a) and soil water content (b) variation during the 2019 growing season (vertical lines represent measurements dates).

The tailings dump soils are characterized by high acidity (pH 3.2) and missing organic components [9,36].

2.2. Gas Exchange Measurements

Gas exchange during photosynthesis was measured using a portable photosynthesis system (LI-6800, LI-COR Inc., Lincoln, NE, USA) equipped with a standard infrared gas-exchange analyser (IRGA) and a chamber for broadleaf species (area: 6 cm²). Instantaneous gas exchange was recorded at three time points in 2019 (29–30 June, 30–31 July and 30–31 August) between 9 am and 3 pm. Measurements, at each time point during the season, were performed on one leaf from five different exemplars of each broadleaf species: green alder, birch, aspen and goat willow. Due to difficult site accessibility (high mountain and degraded land) and the long time required for measurement (multiple dead times for stabilization and between measurements), we extended the day measurement period by

3 h, compared with the standard practice. We planned the experiment, in order to minimize the influence of diurnal variability of photosynthesis, by measuring the first exemplar of each species, followed by the second exemplar of each species and so on. We took into consideration that increasing the number of measurement days (now limited to two days for each time point during the season) could induce more variability because climatic parameters can change significantly (e.g., precipitation or temperature).

All studied species have C3 photosynthetic pathways. The selected trees were saplings, with a mean height of 1.5–2.0 m for silver birch, goat willow and aspen and 1.0 m for green alder. Measurements were performed on different leaves from one time point to another, but from the same exemplars. Selected leaves were completely developed, had no damage and were located on the upper part of the crown, in full exposure to light.

Instrument calibration was performed at the start of each session following the manufacturer's recommendations [38]. To assure measurement accuracy, the gas analyser was matched when the following conditions were met: elapsed time since the last match >10 min, CO₂ measured by the reference analyser have changed by 100 μmol·mol⁻¹ since the last match, difference between CO₂ reference and CO₂ sample <10 μmol·mol⁻¹, and difference in H₂O <1 mmol·mol⁻¹. While collecting the measurements, the mean temperature and relative humidity in the measurement chamber were 22.3 ± 1.8 °C and 60 ± 1.2%, respectively, the fan speed was 10,000 rpm and the flow rate was 500 μmol·s⁻¹. The irradiance photosynthetic photon flux density (PPFD) was set to 1000 μmol·m⁻²·s⁻¹ and was kept constant for all measurements, with following light composition ratio of 0.9 red and 0.1 blue using the LI-COR 6800 light source.

To obtain response curves for net photosynthetic rate as a function of intercellular CO₂ concentration, a chamber CO₂ gradient consisting of 400, 200, 100, 50, 400, 600, 800, 1000, and 1200 μmol·mol⁻¹ was used. Response curve measurements were performed on one leaf from five different exemplars for each species. Between each measurement time point during the season, the exemplars were kept the same, but the leaves differ. Steady-state values from each leaf at different CO₂ concentrations were recorded after 2–3 min, an interval which allowed the leaf to adjust to the new environmental conditions (a stability point was reached when the standard deviation for CO₂ and H₂O differences was ≤0.1 for 20 s) [38,39].

Light-saturated net photosynthetic rate A (μmol CO₂·m⁻²·s⁻¹), transpiration rate E (mmol H₂O·m⁻²·s⁻¹), stomatal conductance to water vapour g_{sw} (mol H₂O·m⁻²·s⁻¹), and intercellular CO₂ concentration C_i (μmol·mol⁻¹) and leaf temperature T_{leaf} (°C) were measured. Using these measured parameters, three efficiency parameters were then calculated: water use efficiency WUE (as A/E , μmol CO₂·m⁻²·s⁻¹/mmol H₂O·m⁻²·s⁻¹), intrinsic water use efficiency $iWUE$ (as A/g_{sw} , μmol·mol⁻¹) and instantaneous carboxylation efficiency A/C_i (μmol CO₂·m⁻²·s⁻¹/μmol·mol⁻¹) [40]. During the gas exchange measurements, a uniform distribution of photosynthesis and transpiration over the leaf was assumed [41].

2.3. The Farquhar–Von Caemmerer–Berry Model

Data from the response curve of net photosynthetic rate to CO₂ were analysed using the Farquhar–von Caemmerer–Berry model (the FvCB model) [42]. This model was developed to model leaf gas exchange and net photosynthetic rate (A) for C3 plants under any given environmental conditions. It has been used widely in recent decades to summarise the dependence of carbon assimilation rate on intercellular CO₂ concentration (C_i) because of its simple form and the comparable metrics of photosynthetic capacity that are provided. The net photosynthetic rate predicted by the FvCB model is the minimum between the Rubisco limited rate (A_c), the ribulose 1,5-bisphosphate (RuBP)-regeneration or electron (e-) transport limited rate (A_j) and the triose phosphate utilization (TPU) limited rate (A_p) of CO₂ assimilation [43,44]. Considering the three limitation phases, the net photosynthetic rate can be modelled as follows:

$$A = \min(A_c, A_j, A_p) \quad (1)$$

In the Rubisco limited phase, the response of net assimilation (A_c) to C_i is defined by:

$$A_c = \frac{V_{cmax} * (C_i - \Gamma^*)}{C_i + K_C * (1 + O/K_O)} - R_d \quad (2)$$

where R_d is day respiration ($\mu\text{mol}\cdot\text{m}^{-2}\cdot\text{s}^{-1}$), V_{cmax} is the maximum carboxylation rate of Rubisco ($\mu\text{mol}\text{CO}_2\cdot\text{m}^{-2}\cdot\text{s}^{-1}$), Γ^* is the photosynthetic compensation point ($\mu\text{mol}\cdot\text{mol}^{-1}$), K_C is the Michaelis–Menten constant of Rubisco for CO_2 ($\mu\text{mol}\cdot\text{mol}^{-1}$), K_O is the Michaelis–Menten constant of Rubisco for O_2 ($\mu\text{mol}\cdot\text{mol}^{-1}$), and O is the intercellular partial pressure of O_2 ($\text{mmol}\cdot\text{mol}^{-1}$) set to 21 KPa.

During the RuBP-regeneration or electron transport, the response of net assimilation (A_j) to C_i is defined by:

$$A_j = \frac{J * (C_c - \Gamma^*)}{4C_c + 8\Gamma^*} - R_d \quad (3)$$

where J is the rate of electron transport ($\mu\text{mol}\cdot\text{e}^{-1}\cdot\text{m}^{-2}\cdot\text{s}^{-1}$).

In the TPU limited phase, the net assimilation rate (A_p) is defined as:

$$A_p = 3T_p - R_d \quad (4)$$

where T_p is the rate of phosphate release in triose phosphate utilization ($\mu\text{mol}\cdot\text{m}^{-2}\cdot\text{s}^{-1}$).

The kinetic constants of Rubisco (Γ^* , K_C , K_O), which are temperature-dependent, were derived using Arrhenius-type equations using the leaf temperature measurements [45,46]. Traits of photosynthetic capacity (V_{cmax} , J_{max} , TPU) were derived from the FvCB model and were corrected to a temperature of 25 °C [47]. More information and details about A/C_i data fitting can be found in the literature [48–50]. The FvCB model was applied for each leaf, and coefficients were analysed as mean.

2.4. Data Analyses

Differences between species were analysed using ANOVA followed by post hoc Tukey tests [51]. The dependence between photosynthetic parameters was quantified using the Pearson correlation coefficient. Statistical tests were considered significant at the $p < 0.05$ level. FvCB model parameters were estimated using the R package ‘plantecophys’ [47], and figures were constructed using the packages ‘ggplot2’ and ‘cowplot’. All data processing was done using R 4.0.3 software [52].

3. Results and Discussion

3.1. Photosynthetic Parameters for Deciduous Pioneer Species

To compare the eco-physiological performance of the deciduous pioneer species that naturally colonized the mining dump areas in the Călimani Mountains, the mean values of photosynthetic traits during the 2019 vegetation period were analysed for CO_2 concentration close to the actual environmental concentration ($400\ \mu\text{mol}\cdot\text{mol}^{-1}$).

Green alder and birch had the highest net assimilation rate for the entire season among the four species analysed (Table 1). The lowest net assimilation rate was recorded for goat willow. The net assimilation rate for green alder was significantly higher than those of aspen and goat willow, while the net assimilation rate of birch was significantly different only from that of goat willow. Similar values for net assimilation (ranging from 12.8 to 17.3 $\mu\text{mol}\text{CO}_2\cdot\text{m}^{-2}\cdot\text{s}^{-1}$) have been documented under similar measurement conditions (1400 $\mu\text{mol}\cdot\text{m}^{-2}\cdot\text{s}^{-1}$ PPFD and 320 $\mu\text{mol}\cdot\text{mol}^{-1}$ CO_2 concentration) for the seedlings of different *Alnus* species [33]. However, our results showed slightly higher net assimilation values for silver birch compared with the range reported in the literature [31,32,53].

Table 1. Mean values (\pm standard deviation) of photosynthetic parameters for the 2019 growing season, at 400 $\mu\text{mol}\cdot\text{mol}^{-1}$ CO_2 concentration and 1000 $\mu\text{mol}\cdot\text{m}^{-2}\cdot\text{s}^{-1}$ PPFD. Significant differences are shown using letters following the Tukey test ($p < 0.05$).

Parameters	Green Alder	Birch	Aspen	Goat Willow
A ($\mu\text{mol CO}_2\cdot\text{m}^{-2}\cdot\text{s}^{-1}$)	17.35 \pm 3.62 ^a	16.62 \pm 2.47 ^{ab}	14.43 \pm 2.93 ^{bc}	13.31 \pm 4.97 ^c
E ($\text{mmol H}_2\text{O}\cdot\text{m}^{-2}\cdot\text{s}^{-1}$)	2.6 \pm 0.78 ^a	3.44 \pm 0.94 ^b	2.94 \pm 1.16 ^{ab}	2.75 \pm 1.34 ^{ab}
<i>gsw</i> ($\text{mol H}_2\text{O}\cdot\text{m}^{-2}\cdot\text{s}^{-1}$)	0.24 \pm 0.10 ^a	0.31 \pm 0.08 ^a	0.27 \pm 0.10 ^a	0.25 \pm 0.12 ^a
<i>Ci</i> ($\mu\text{mol}\cdot\text{mol}^{-1}$)	240.76 \pm 26.07 ^a	278.21 \pm 13.61 ^b	272.36 \pm 29.13 ^b	274.16 \pm 24.30 ^b
<i>A/Ci</i> ($\mu\text{mol CO}_2\cdot\text{m}^{-2}\cdot\text{s}^{-1}/\mu\text{mol}\cdot\text{mol}^{-1}$)	0.07 \pm 0.01 ^a	0.06 \pm 0.01 ^b	0.05 \pm 0.01 ^{bc}	0.05 \pm 0.02 ^c
WUE ($\mu\text{mol CO}_2\cdot\text{m}^{-2}\cdot\text{s}^{-1}/\text{mmol H}_2\text{O}\cdot\text{m}^{-2}\cdot\text{s}^{-1}$)	6.92 \pm 1.08 ^a	5.07 \pm 1.09 ^b	5.63 \pm 2.07 ^b	5.49 \pm 1.78 ^b
iWUE ($\mu\text{mol}\cdot\text{mol}^{-1}$)	78.05 \pm 18.91 ^a	54.92 \pm 8.85 ^b	60.93 \pm 20.73 ^b	60.9 \pm 18.41 ^b

Birch had the highest rates of transpiration and stomatal conductance. The rates of transpiration for birch were significantly higher than those for green alder, but stomatal conductance was not significantly different between species. Similar transpiration rate (3.4 $\text{mmol}\cdot\text{m}^{-2}\cdot\text{s}^{-1}$) and stomatal conductance (0.4 $\text{mol}\cdot\text{m}^{-2}\cdot\text{s}^{-1}$) have been observed for mountain birch at the treeline on the Tibetan Plateau [54]. Birch proveniences and leaf types (early vs. late leaves) can induce differences in stomatal conductance [12].

Diffusion of CO_2 into the intercellular spaces inside leaves occurs mainly through stomatal pores [55]. Stomatal density and distribution on leaves differ among species. As a result, we obtained different *Ci* values even though the CO_2 concentration in the measurement chamber (400 $\mu\text{mol}\cdot\text{mol}^{-1}$) was similar for all species. Green alder had the lowest intercellular CO_2 concentration, which was significantly different from those of the other species. The variation in intercellular CO_2 concentration allows us to understand whether the decline in net photosynthesis rate is due to stomatal limitations or to the reduction of photosynthetic activity in the leaves' cells [56].

Instantaneous carboxylation efficiency was the lowest for aspen and goat willow and the highest for green alder. This photosynthetic parameter can be considered as an estimate of Rubisco activity; generally, higher intercellular CO_2 concentration is associated with lower stomatal conductance. Water use efficiency (WUE and iWUE) was also the highest for green alder and differed significantly from those of the other species.

Regardless of the species, the highest correlation was observed between transpiration rate and stomatal conductance (Table 2). For birch only, a negative correlation was found between net assimilation rate and intercellular CO_2 concentration. The correlation coefficient between net assimilation rate and transpiration rate varied from 0.74 (birch) to 0.93 (goat willow) and was significant in all cases. Similar significant negative correlations between *Ci* and *A* have also been found for birch in a Lithuanian forest (boreal zone) [40].

3.2. Variability of Photosynthetic Parameters during the Vegetation Season

For broadleaf species, the chlorophyll content of leaves changes throughout the growing season, which induces variability in eco-physiological processes. Because of these biochemical changes in leaves, it is important to explore the variation in individual photosynthetic parameters during the vegetation season [12]. To avoid the systematic influence of diurnal variation, the gas exchange measurements were distributed during the day from 9 am to 3 pm. The net assimilation rate varied across the season for all four species, with the lowest values recorded at the end of June (Figure 2a). The lowest net assimilation rate was observed for goat willow at the end of June (7.55 $\mu\text{mol CO}_2\cdot\text{m}^{-2}\cdot\text{s}^{-1}$) and was significantly different from the values in other months. For green alder, the maximum value of net assimilation was measured at the end of July (18.64 $\mu\text{mol CO}_2\cdot\text{m}^{-2}\cdot\text{s}^{-1}$), and the minimum was recorded at the end of June (14.93 $\mu\text{mol CO}_2\cdot\text{m}^{-2}\cdot\text{s}^{-1}$). A similar trend in variation was found for goat willow. On the contrary, net assimilation rates for birch and aspen increased continuously during the season.

Table 2. Pearson correlation coefficients for relationships between gas exchange parameters (A —net photosynthetic rate, E —transpiration rate, g_{sw} —stomatal conductance, C_i —intercellular CO_2 concentration).

Parameters	E	g_{sw}	C_i
Green alder			
A	0.80 **	0.87 **	0.73 **
E		0.88 **	0.84 **
g_{sw}			0.93 **
Birch			
A	0.74 **	0.77 **	−0.13
E		0.94 **	0.46 *
g_{sw}			0.52 **
Aspen			
A	0.84 **	0.84 **	0.66 **
E		0.96 **	0.82 **
g_{sw}			0.87 **
Goat willow			
A	0.93 **	0.94 **	0.45 *
E		0.97 **	0.66 **
g_{sw}			0.67 **

** Significance at $p < 0.01$; * Significance at $p < 0.05$.

Studies in boreal forests indicate that, for birch, the highest rates of leaf-mass net assimilation occur under light-saturated conditions in early May after the leaves unfold, and there is minimal variation during the vegetation season [12]. For other species, the maximum leaf-area net assimilation occurs in late June and early July [31]. Studies on different *Salix* spp. have highlighted a weak correlation between biomass yield and photosynthetic rate and a positive influence of total leaf area per plant [27].

Stomatal conductance increased continuously from the beginning of the season to autumn for all species, except goat willow (Figure 2b). A similar pattern was observed for transpiration rate, but with a higher rate of increase from the beginning to the end of the season. These two parameters had a similar trend in variation because transpiration is regulated mainly by stomatal conductance [56]. The stomatal conductance of aspen and goat willow in June was significantly different from that measured in July or August. The maximum values for transpiration rate were measured in August for green alder ($2.96 \text{ mmol H}_2\text{O}\cdot\text{m}^{-2}\cdot\text{s}^{-1}$), aspen ($3.93 \text{ mmol H}_2\text{O}\cdot\text{m}^{-2}\cdot\text{s}^{-1}$) and birch ($4.22 \text{ mmol H}_2\text{O}\cdot\text{m}^{-2}\cdot\text{s}^{-1}$) and in July for goat willow ($3.35 \text{ mmol H}_2\text{O}\cdot\text{m}^{-2}\cdot\text{s}^{-1}$) (Figure 2c).

iWUE and WUE decreased during the vegetation season for all studied species, possibly linked with the lower soil water content during the measurements in July and August (see Figure 1). Water use efficiency parameters were significantly different between all three measurement timepoints only in the case of aspen. Similarly, differences between monthly values of WUE have been reported for another poplar species (*Populus angustifolia*) from North America [57]. Goat willow exhibited a different trend in variation, with slightly higher iWUE values at the end of August compared to July. Green alder had the highest values of both WUE and iWUE compared to other species.

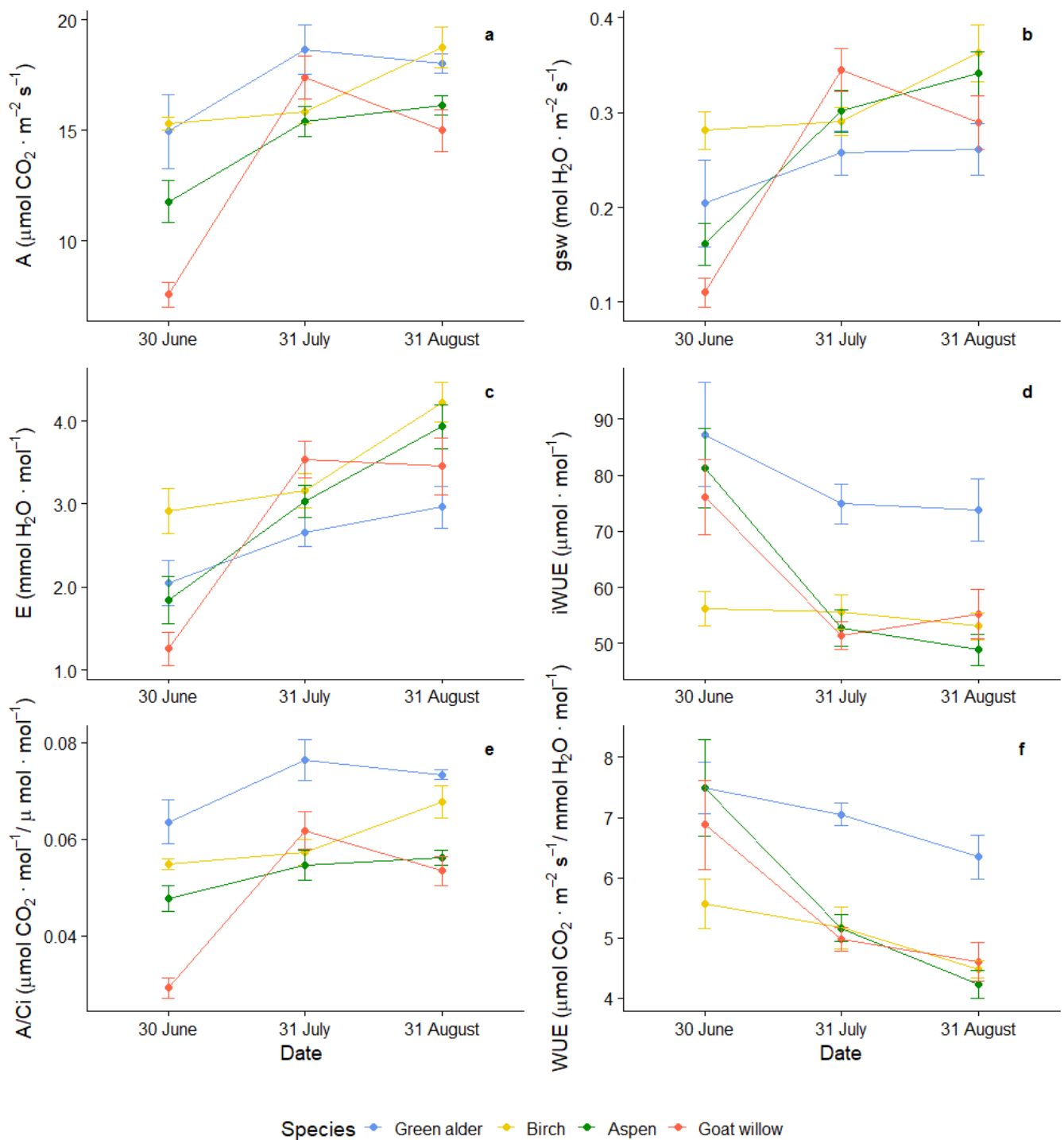


Figure 2. Variability in photosynthetic parameters during the 2019 growing season for deciduous pioneer species on a tailing dump in the Călimani Mountains. (a) Net assimilation rate, (b) stomatal conductance, (c) transpiration rate, (d) intrinsic water use efficiency, (e) instantaneous carboxylation efficiency, (f) water use efficiency (points are mean values, and whiskers represent standard errors).

Variation in iWUE and WUE during the season is a consequence of both changing environmental conditions and physiological changes in leaf structure due to ageing [58]. Both parameters reflect water use efficiency (how much carbon is fixed per unit of water loss), but WUE can also be used as a water stress indicator (drought indicator) [59]. Higher values of iWUE or WUE can be achieved through lower stomatal conductance or transpiration rate, higher assimilation capacity or a combination of both [60]. Water supply is one factor that can cause plants to have a lower stomatal conductance and higher WUE [12]. Our study was conducted in a mountain area where precipitation is not a limiting factor, but variations in WUE may still occur due to particular conditions induced by precipitation variation during vegetation season. In the second and third measurement time points, low soil water content was reported (see Figure 1), which may induce a decrease in water use efficiency parameters.

Green alder also demonstrated the highest instantaneous carboxylation efficiency compared with other deciduous pioneer species, with a maximum in late July (Figure 2e). It had a lower intercellular CO₂ concentration but maximum values for assimilation rate. One possible explanation for this is that green alder is in its optimal distribution range, is acclimatized to cold environments and uses resources more efficiently. The maximum instantaneous carboxylation efficiency occurred in July for goat willow and at the end of August for aspen and birch.

The mining dump areas are exposed to high light intensity, large temperature variability and low nitrogen availability. Low availability of soil nitrogen can be an important limiting factor of photosynthesis [19,21]. N₂-fixing plants that are capable of fixing atmospheric nitrogen, like green alder, can be more performant in terms of photosynthetic traits on degraded soils compared with other pioneer species [61]. Leaf size and structure, combined with crown size and branching patterns, play an important role in the assimilation performance of different species [62]. Field observations confirm that the leaf area and crown development of green alder are greater than for the other species.

3.3. Photosynthesis Response Curve under Increasing CO₂ Concentration

Using a variable concentration of CO₂ to understand assimilation performance is more efficient than using a constant CO₂ concentration [63]. An *A/C_i* curve can be constructed to understand and interpret the biochemical processes of leaf photosynthesis under various environmental conditions. The measured values of net assimilation at different CO₂ concentrations are used to estimate photosynthetic limitations and parameters of photosynthetic performance using two key parameters from the FvCB model: V_{cmax} and J_{max} .

The response curve for the relationship between assimilation and CO₂ concentration shows an initial increase followed by a relatively constant variation caused by light limitation (Figure 3). A clear difference between the three measurement time points was observed for all species, except for birch in June and July. The limitation of assimilation rate due to light availability occurred after reaching an intercellular CO₂ concentration of 500 $\mu\text{mol}\cdot\text{mol}^{-1}$. After passing this threshold, the highest assimilation rate was measured in August for all four species. For goat willow and aspen, variation in WUE in relation to CO₂ concentration was higher in June.

Based on the FvCB model, the limitations of the photosynthetic process are characterized by two main parameters— V_{cmax} and J_{max} —and occasionally also by TPU. Estimation of these parameters is regulated by the limitations of one of three curves of the FvCB model. V_{cmax} is the maximum rate of Rubisco activity and reflects a limitation in RuBP-regeneration [48]. For green alder, the highest values of V_{cmax} were recorded in July, and the lowest in June, without significant differences during the season (Figure 4a). For birch and aspen, there were no significant differences in V_{cmax} during the season. The lowest V_{cmax} for goat willow was recorded in June, statistically different from the rest of the season, and was associated with lower assimilation levels. To derive the seasonal mean of V_{cmax} , it is recommended to perform measurements in midsummer. Maximum values of V_{cmax} were obtained in the middle of the vegetation season (end July).

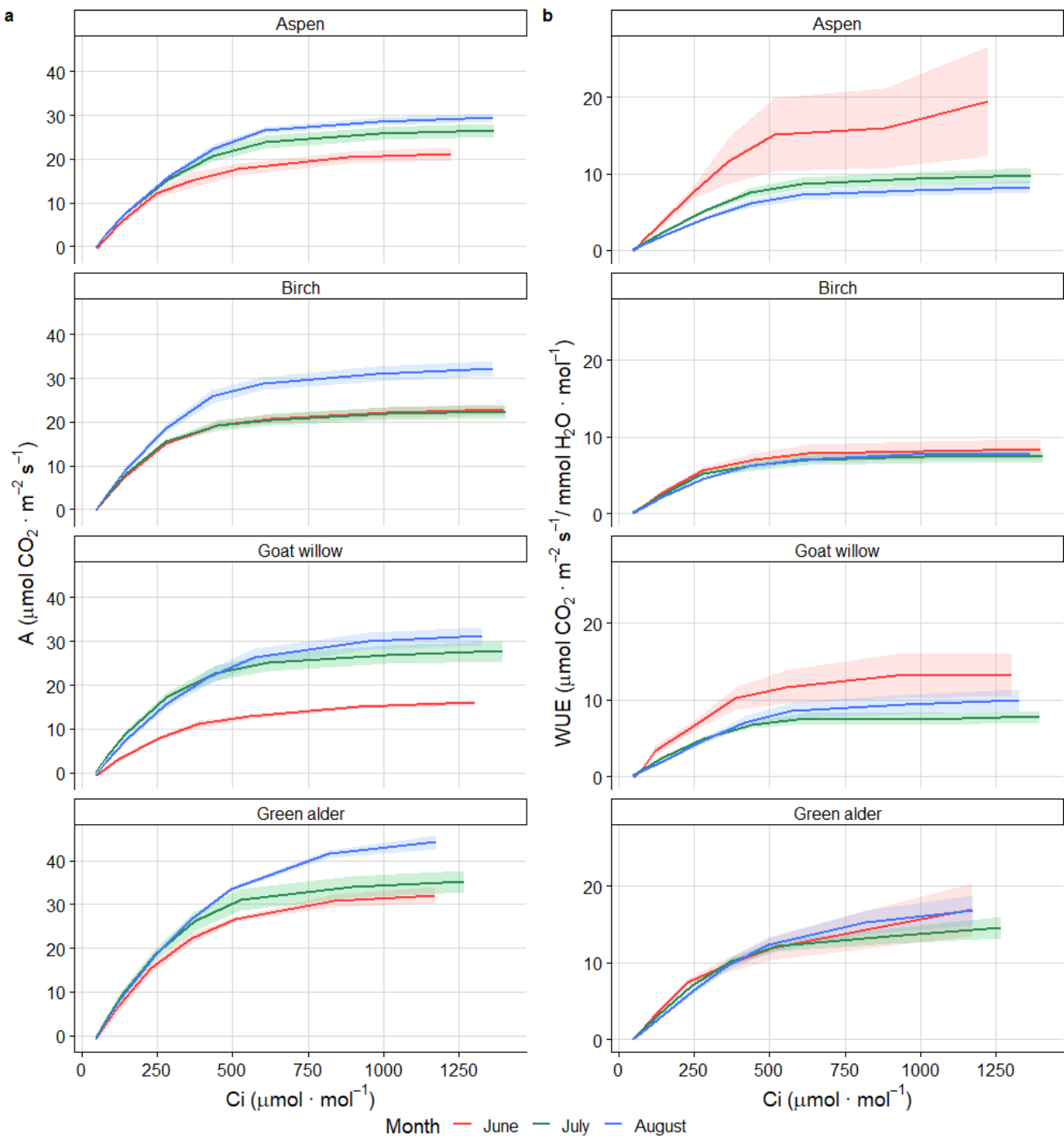


Figure 3. (a) Mean response curve of net assimilation relative to intercellular CO_2 concentration as modelled by the FvCB model; (b) water use efficiency relative to intercellular CO_2 concentration (shaded areas represent standard error).

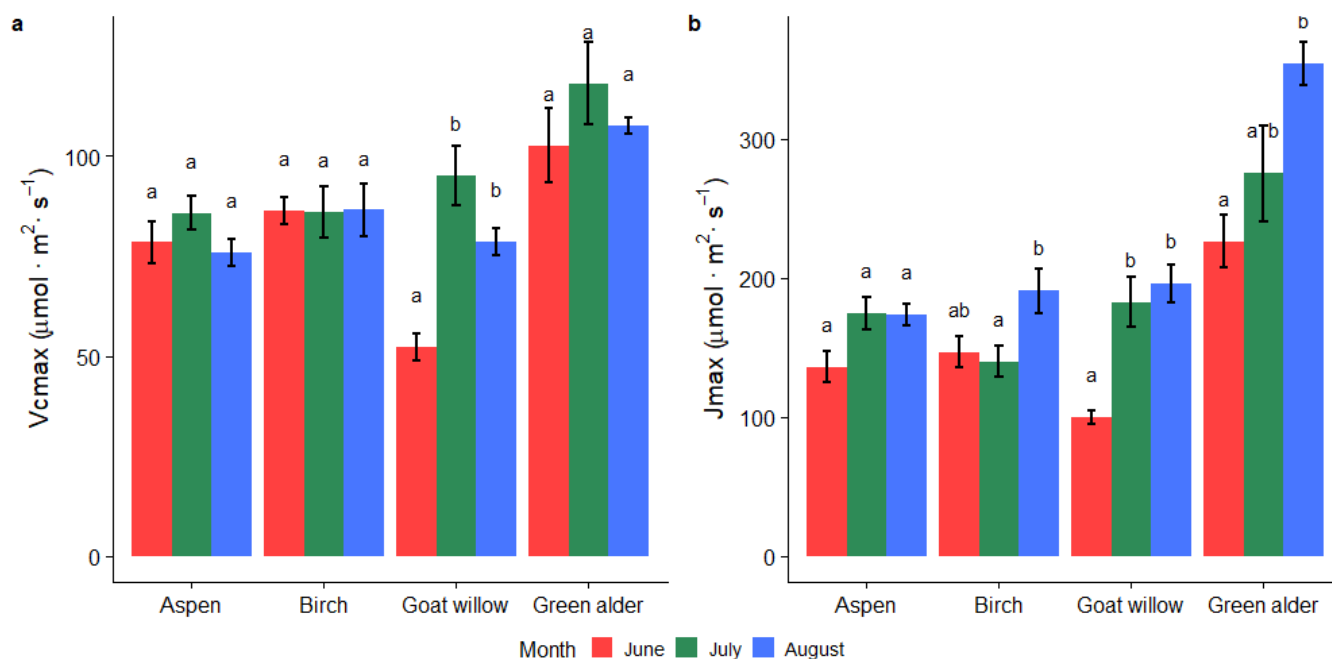


Figure 4. Mean values of FvCB model parameters for deciduous pioneer species on tailings dumps in the Călimani Mountains: (a) V_{cmax} —maximum rate of Rubisco activity; (b) J_{max} —maximum rate of electron transport for RuPB-regeneration (whiskers represent standard errors, and letters represent significant differences).

J_{max} represents the maximum rate of electron transport for RuPB-regeneration at the light intensity used in the study ($1000 \mu\text{mol} \cdot \text{m}^{-2} \cdot \text{s}^{-1}$) (Figure 4b) [64]. J_{max} was the lowest in June and highest in August, regardless of the species. With exception of aspen, the J_{max} differs significantly between time points during the season. V_{cmax} and J_{max} are correlated with A_{max} (the maximum value of assimilation) because these parameters all reflect limitations in photosynthetic processes. Green alder exhibited the highest values of V_{cmax} and J_{max} and also had the highest rate of photosynthesis at both ambient and saturating CO_2 , while goat willow presented the lowest values for all of these variables. The ratio of J_{max} to V_{cmax} varied in the typical range (1.5 to 2.5) observed for other woody species [65].

TPU limitation occurred in less than half of the samples, as it generally requires a higher C_i concentration than that used in our study. This third state of photosynthesis limitation occurs when the chloroplast system's reaction is greater than the possibility of the leaf using the triose phosphate [43]. This is more likely to happen under experimental conditions than in natural situations, and this limitation state has not been taken into account in many studies [66].

Light dependence of J_{max} varied by up to 40% across the different leaves of birch [30]. Meanwhile, V_{cmax} is dependent on the temperature and increases at higher temperatures, but with limitations at very high temperatures [30]. For *Populus* species, multiple studies have documented V_{cmax} and J_{max} values lower than those reported in this study, even though the light radiance used was higher, at $200\text{--}500 \mu\text{mol} \cdot \text{m}^{-2} \cdot \text{s}^{-1}$ [25]. A global study that analysed more than 350 species highlighted that, for tree species, the mean values of V_{cmax} and J_{max} were $66.6 \mu\text{mol} \cdot \text{m}^{-2} \cdot \text{s}^{-1}$ and $114.4 \mu\text{mol} \cdot \text{m}^{-2} \cdot \text{s}^{-1}$, respectively [67].

4. Conclusions

Reforestation and the stable ecological restoration of tailings dumps resulting from surface mining activities in the Călimani Mountains have been a high priority for regional and national administrations in the last two decades. Even though several solutions have been implemented (dumps stabilization, soil amendments, etc.), the complete recovery

of the degraded habitats is still a challenge. Gaining a better understanding of natural colonization with pioneer woody species, such as through studying primary natural succession, can offer valuable knowledge about the species that are most adapted to these particular environmental conditions.

The most productive pioneer species in terms of photosynthetic traits was the green alder, a woody N₂-fixing shrub. It showed the highest rates of net assimilation, carboxylation efficiency and water use efficiency and can be a suitable species for reforestation based on the study conditions. During the growing season, this species' maximum photosynthetic capacity is generally observed at the end of July, with a minimum in late June.

A detailed understanding of the variability and dynamics of the photosynthetic capacity of pioneer species that naturally occur on tailings dumps is essential, offering valuable data to the process of characterizing suitable species for ecological restoration systems to heal these open wounds in the landscape.

Author Contributions: Conceptualization, I.P. and A.P.; methodology, A.P.; writing—original draft preparation, A.P.; writing—review and editing, I.P. All authors have read and agreed to the published version of the manuscript.

Funding: This research was funded by the Romanian Ministry of Research and Innovation in Core Program for forestry—BIOSERV (2019)—Project PN 19070102.

Data Availability Statement: Data is available on request formed to the corresponding author.

Acknowledgments: We thank Margareta Grudnicki for valuable suggestions and the Forestry Faculty of Suceava for supporting this study.

Conflicts of Interest: The authors declare no conflict of interest.

References

- Shukla, P.R.; Skea, J.; Buendia, E.C.; Masson-Delmotte, V.; Pörtner, H.-O.; Roberts, D.C.; Zhai, P.; Slade, R.; Connors, S.; van Diemen, R.; et al. *IPCC, 2019: Climate Change and Land: An IPCC Special Report on Climate Change, Desertification, Land Degradation, Sustainable Land Management, Food Security, and Greenhouse Gas Fluxes in Terrestrial Ecosystems*; Intergovernmental Panel on Climate Change (IPCC): Geneva, Switzerland, 2019; pp. 1–864.
- Liu, S.; Li, W.; Qiao, W.; Wang, Q.; Hu, Y.; Wang, Z. Effect of Natural Conditions and Mining Activities on Vegetation Variations in Arid and Semiarid Mining Regions. *Ecol. Indic.* **2019**, *103*, 331–345. [[CrossRef](#)]
- Chauhan, S.S. Mining, Development and Environment: A Case Study of Bijolia Mining Area in Rajasthan, India. *J. Hum. Ecol.* **2010**, *31*, 65–72. [[CrossRef](#)]
- Deng, J.; Bai, X.; Zhou, Y.; Zhu, W.; Yin, Y. Variations of Soil Microbial Communities Accompanied by Different Vegetation Restoration in an Open-Cut Iron Mining Area. *Sci. Total Environ.* **2020**, *704*, 135243. [[CrossRef](#)] [[PubMed](#)]
- Henry, H.F.; Burken, J.G.; Maier, R.M.; Newman, L.A.; Rock, S.; Schnoor, J.L.; Suk, W.A. Phytotechnologies—Preventing Exposures, Improving Public Health. *Int. J. Phytoremediat.* **2013**, *15*, 889–899. [[CrossRef](#)] [[PubMed](#)]
- Macdonald, S.E.; Landhäusser, S.M.; Skousen, J.; Franklin, J.; Frouz, J.; Hall, S.; Jacobs, D.F.; Quideau, S. Forest Restoration Following Surface Mining Disturbance: Challenges and Solutions. *New For.* **2015**, *46*, 703–732. [[CrossRef](#)]
- Pietrzykowski, M. Tree Species Selection and Reaction to Mine Soil Reconstructed at Reforested Post-Mine Sites: Central and Eastern European Experiences. *Ecol. Eng. X* **2019**, *3*, 100012. [[CrossRef](#)]
- Frouz, J.; Dvorščák, P.; Vávrová, A.; Doušová, O.; Kadochová, Š.; Matějček, L. Development of Canopy Cover and Woody Vegetation Biomass on Reclaimed and Unreclaimed Post-Mining Sites. *Ecol. Eng.* **2015**, *84*, 233–239. [[CrossRef](#)]
- Cenușă, E. *Instalarea Vegetației Naturale În Zone Afectate de Activități Miniere Din Parcul National Călimani*; Forestry Technical Publishing House: Voluntari, Romania, 2018.
- Boscutti, F.; Poldini, L.; Buccheri, M. Green Alder Communities in the Alps: Phytosociological Variability and Ecological Features. *Plant Biosyst.* **2014**, *148*, 917–934. [[CrossRef](#)]
- Mauri, A.; Caudullo, G. *Alnus viridis* in Europe: Distribution, Habitat, Usage and Threats. In *European Atlas of Forest Tree Species*; European Commission: Brussels, Belgium, 2016; p. 68. [[CrossRef](#)]
- Tenkanen, A.; Keski-Saari, S.; Salojärvi, J.; Oksanen, E.; Keinänen, M.; Kontunen-Soppela, S. Differences in Growth and Gas Exchange between Southern and Northern Provenances of Silver Birch (*Betula pendula* Roth) in Northern Europe. *Tree Physiol.* **2020**, *40*, 198–214. [[CrossRef](#)]
- Beck, P.; Caudullo, G.; de Rigo, D.; Tinner, W. *Betula pendula*, *Betula pubescens* and Other Birches in Europe: Distribution, Habitat, Usage and Threats. In *European Atlas of Forest Tree Species*; European Commission: Brussels, Belgium, 2016; pp. 70–73. [[CrossRef](#)]
- Caudullo, G.; de Rigo, D. *Populus tremula* in Europe: Distribution, Habitat, Usage and Threats. In *European Atlas of Forest Tree Species*; European Commission: Brussels, Belgium, 2016; pp. 138–139. [[CrossRef](#)]

15. Enescu, C.M.; Houston Durrant, T.; de Rigo, D.; Caudullo, G. *Salix caprea* in Europe: Distribution, Habitat, Usage and Threats. In *European Atlas of Forest Tree Species*; European Commission: Brussels, Belgium, 2016; pp. 170–171. [[CrossRef](#)]
16. Pallardy, S. Physiology of Woody Plants. *Pac. Conserv. Biol.* **1998**, *4*, 272. [[CrossRef](#)]
17. Cavaleri, M.A.; Reed, S.C.; Smith, W.K.; Wood, T.E. Urgent Need for Warming Experiments in Tropical Forests. *Glob. Chang. Biol.* **2015**, *21*, 2111–2121. [[CrossRef](#)]
18. Long, S.P.; Bernacchi, C.J. Gas Exchange Measurements, What Can They Tell Us about the Underlying Limitations to Photosynthesis? Procedures and Sources of Error. *J. Exp. Bot.* **2003**, *54*, 2393–2401. [[CrossRef](#)] [[PubMed](#)]
19. Zhao, X.; Mao, Z.; Xu, J. Gas Exchange, Chlorophyll and Growth Responses of *Betula Platyphylla* Seedlings to Elevated CO₂ and Nitrogen. *Int. J. Biol.* **2010**, *2*, 143–149. [[CrossRef](#)]
20. Liu, M.Z.; Jiang, G.M.; Li, Y.G.; Gao, L.M.; Niu, S.L.; Cui, H.X.; Ding, L. Gas Exchange, Photochemical Efficiency, and Leaf Water Potential in Three *Salix* Species. *Photosynthetica* **2003**, *41*, 393–398. [[CrossRef](#)]
21. Bojarczuk, K.; Karolewski, P.; Oleksyn, J.; Kieliszewska-Rokicka, B.; Zytковиak, R.; Tjoelker, M.G. Effect of Polluted Soil and Fertilisation on Growth and Physiology of Silver Birch (*Betula pendula* Roth.) Seedlings. *Polish J. Environ. Stud.* **2002**, *11*, 483–492.
22. Hermle, S.; Vollenweider, P.; Günthardt-Goerg, M.S.; Mcquattie, C.J.; Matyssek, R. Leaf Responsiveness of *Populus tremula* and *Salix viminalis* to Soil Contaminated with Heavy Metals and Acidic Rainwater. *Tree Physiol.* **2007**, *27*, 1517–1531. [[CrossRef](#)] [[PubMed](#)]
23. Han, G.; Cui, B.X.; Zhang, X.X.; Li, K.R. The Effects of Petroleum-Contaminated Soil on Photosynthesis of *Amorpha fruticosa* Seedlings. *Int. J. Environ. Sci. Technol.* **2016**, *13*, 2383–2392. [[CrossRef](#)]
24. Horton, J.L.; Kolb, T.E.; Hart, S.C. Leaf Gas Exchange Characteristics Differ among Sonoran Desert Riparian Tree Species. *Tree Physiol.* **2001**, *21*, 233–241. [[CrossRef](#)]
25. Zhu, G.F.; Li, X.; Su, Y.H.; Huang, C.L. Parameterization of a Coupled CO₂ and H₂O Gas Exchange Model at the Leaf Scale of *Populus euphratica*. *Hydrol. Earth Syst. Sci.* **2010**, *14*, 419–431. [[CrossRef](#)]
26. Rood, S.B.; Nielsen, J.L.; Shenton, L.; Gill, K.M.; Letts, M.G. Effects of Flooding on Leaf Development, Transpiration, and Photosynthesis in Narrowleaf Cottonwood, a Willow-like Poplar. *Photosynth. Res.* **2010**, *104*, 31–39. [[CrossRef](#)]
27. Andralojc, P.J.; Bencze, S.; Madgwick, P.J.; Philippe, H.; Powers, S.J.; Shield, I.; Karp, A.; Parry, M.A.J. Photosynthesis and Growth in Diverse Willow Genotypes. *Food Energy Secur.* **2014**, *3*, 69–85. [[CrossRef](#)]
28. Talbot, R.J.; Etherington, J.R.; Bryant, J.A. Comparative Studies of Plant Growth and Distribution in Relation to Waterlogging. XII. Growth, Photosynthetic Capacity and Metal Ion Uptake in *Salix Caprea* and *S. Cinerea* Ssp. *Oleifolia*. *New Phytol.* **1987**, *105*, 563–574. [[CrossRef](#)]
29. Johnson, J.D.; Tognetti, R.; Paris, P. Water Relations and Gas Exchange in Poplar and Willow under Water Stress and Elevated Atmospheric CO₂. *Physiol. Plant.* **2002**, *115*, 93–100. [[CrossRef](#)]
30. Aalto, T.; Juurola, E. Parametrization of a Biochemical CO₂ Exchange Model for Birch (*Betula pendula* Roth.). *Boreal Environ. Res.* **2001**, *6*, 53–64.
31. Oleksyn, J.; Żytковиak, R.; Reich, P.B.; Tjoelker, M.G.; Karolewski, P. Ontogenetic Patterns of Leaf CO₂ Exchange, Morphology and Chemistry in *Betula Pendula* Trees. *Trees Struct. Funct.* **2000**, *14*, 271–281. [[CrossRef](#)]
32. Hoshika, Y.; Watanabe, M.; Inada, N.; Mao, Q.; Koike, T. Photosynthetic Response of Early and Late Leaves of White Birch (*Betula platyphylla* Var. *Japonica*) Grown under Free-Air Ozone Exposure. *Environ. Pollut.* **2013**, *182*, 242–247. [[CrossRef](#)]
33. Côté, B.; Carlson, R.W.; Dawson, J.O. Leaf Photosynthetic Characteristics of Seedlings of Actinorhizal *Alnus* Spp. and *Elaeagnus* Spp. *Photosynth. Res.* **1988**, *16*, 211–218. [[CrossRef](#)]
34. Piper, F.I.; Cavieres, L.A. Gas Exchange of Juvenile and Mature Trees of *Alnus jorullensis* (Betulaceae) at Sites with Contrasting Humidity in the Venezuelan Andes. *Ecol. Res.* **2010**, *25*, 51–58. [[CrossRef](#)]
35. Popa, A.; Popa, I. Caracteristici ale procesului de fotosinteză la aninul verde din Munții Călimani. *Rev. Silv. Cinegetică* **2019**, *44*, 20–23.
36. Gorea, D.; Hancu, G.; Rusu, A.; Cârje, A.; Barabás, E. Quality Assessment Indicators of Surface Waters and Soils in the Vicinity of the Former Sulfur Mine in the Călimani Mountains. *Forum Geogr.* **2014**, *XIII*, 212–218. [[CrossRef](#)]
37. Erzberger, P.; Höhn, M.; Pócs, T. Contribution to the Bryoflora of Călimani Mountains in the Eastern Carpathians, Romania, I. *Acta Biol. Plant. Agriensis* **2012**, *2*, 75–97.
38. LI-COR. *Using the LI-6800 Portable Photosynthesis System for Bluestem OSTM Version 1.3*; Li-Cor Biosciences: Lincoln, NE, USA, 2018; Volume 1.
39. Covshoff, S. *Photosynthesis Methods and Protocols*; Humana Press: Totowa, NJ, USA, 2018; Volume 1770. [[CrossRef](#)]
40. Marozas, V.; Augustaitis, A.; Pivoras, A.; Baumgarten, M.; Mozgeris, G.; Sasnauskienė, J.; Dautartė, A.; Abraitienė, J.; Bičenkienė, S.; Mordas, G.; et al. Comparative Analyses of Gas Exchange Characteristics and Chlorophyll Fluorescence of Three Dominant Tree Species during the Vegetation Season in Hemi-Boreal Zone, Lithuania. *J. Agric. Meteorol.* **2019**, *75*, 3–12. [[CrossRef](#)]
41. Terashima, I. Anatomy of Non-Uniform Leaf Photosynthesis. *Photosynth. Res.* **1992**, *31*, 195–212. [[CrossRef](#)] [[PubMed](#)]
42. Farquhar, G.D.; von Caemmerer, S.; Berry, J.A. A Biochemical Model of Photosynthetic CO₂ Assimilation in Leaves of C₃ Species. *Planta* **1980**, *149*, 78–90. [[CrossRef](#)] [[PubMed](#)]
43. Sharkey, T.D.; Bernacchi, C.J.; Farquhar, G.D.; Singaas, E.L. Fitting Photosynthetic Carbon Dioxide Response Curves for C₃ Leaves. *Plant Cell Environ.* **2007**, *30*, 1035–1040. [[CrossRef](#)] [[PubMed](#)]

44. Yin, X.; Struik, P.C.; Romero, P.; Harbinson, J.; Evers, J.B.; Van Der Putten, P.E.L.; Vos, J. Using Combined Measurements of Gas Exchange and Chlorophyll Fluorescence to Estimate Parameters of a Biochemical C₃ Photosynthesis Model: A Critical Appraisal and a New Integrated Approach Applied to Leaves in a Wheat (*Triticum aestivum*) Canopy. *Plant Cell Environ.* **2009**, *32*, 448–464. [[CrossRef](#)] [[PubMed](#)]
45. Medlyn, B.E.; Dreyer, E.; Ellsworth, D.; Forstreuter, M.; Harley, P.C.; Kirschbaum, M.U.F.; Le Roux, X.; Montpied, P.; Strassemeyer, J.; Walcroft, A.; et al. Temperature Response of Parameters of a Biochemically Based Model of Photosynthesis. II. A Review of Experimental Data. *Plant Cell Environ.* **2002**, *25*, 1167–1179. [[CrossRef](#)]
46. Bernacchi, C.J.; Singsaas, E.L.; Pimentel, C.; Portis, A.R.; Long, S.P. Improved Temperature Response Functions for Models of Rubisco-Limited Photosynthesis. *Plant Cell Environ.* **2001**, *24*, 253–259. [[CrossRef](#)]
47. Duursma, R.A. Plantecophys—An R Package for Analysing and Modelling Leaf Gas Exchange Data. *PLoS ONE* **2015**, *10*, 1–13. [[CrossRef](#)] [[PubMed](#)]
48. Dubois, J.J.B.; Fiscus, E.L.; Booker, F.L.; Flowers, M.D.; Reid, C.D. Optimizing the Statistical Estimation of the Parameters of the Farquhar-von Caemmerer-Berry Model of Photosynthesis. *New Phytol.* **2007**, *176*, 402–414. [[CrossRef](#)]
49. Yin, X.; Struik, P.C. Theoretical Reconsiderations When Estimating the Mesophyll Conductance to CO₂ Diffusion in Leaves of C₃ Plants by Analysis of Combined Gas Exchange and Chlorophyll Fluorescence Measurements. *Plant Cell Environ.* **2009**, *32*, 1513–1524. [[CrossRef](#)] [[PubMed](#)]
50. Moualeu-Ngangue, D.P.; Chen, T.W.; Stützel, H. A New Method to Estimate Photosynthetic Parameters through Net Assimilation Rate—intercellular Space CO₂ Concentration (A–C_i) Curve and Chlorophyll Fluorescence Measurements. *New Phytol.* **2017**, *213*, 1543–1554. [[CrossRef](#)] [[PubMed](#)]
51. Abdi, H.; Williams, L.J. Tukey’s Honestly Significant Difference (HSD) Test. *Encycl. Res. Des.* **2010**, *3*, 1–5.
52. R Core Team. *A Language and Environment for Statistical Computing*; R Foundation for Statistical Computing: Vienna, Austria, 2019; Available online: <https://www.R-project.org> (accessed on 2 May 2021).
53. Maurer, S.; Matyssek, R. Nutrition and the Ozone Sensitivity of Birch (*Betula pendula*) II. Carbon Balance, Water-Use Efficiency and Nutritional Status of the Whole Plant. *Trees Struct. Funct.* **1997**, *12*, 11–20. [[CrossRef](#)]
54. Xu, Z.; Hu, T.; Zhang, Y. Effects of Experimental Warming on Phenology, Growth and Gas Exchange of Treeline Birch (*Betula utilis*) Saplings, Eastern Tibetan Plateau, China. *Eur. J. For. Res.* **2012**, *131*, 811–819. [[CrossRef](#)]
55. Hanson, D.T.; Stutz, S.S.; Boyer, J.S. Why Small Fluxes Matter: The Case and Approaches for Improving Measurements of Photosynthesis and (Photo)Respiration. *J. Exp. Bot.* **2016**, *67*, 3027–3039. [[CrossRef](#)] [[PubMed](#)]
56. Collatz, G.J.; Ball, J.T.; Grivet, C.; Berry, J.A. Physiological and Environmental Regulation of Stomatal Conductance, Photosynthesis and Transpiration: A Model That Includes a Laminar Boundary Layer. *Agric. For. Meteorol.* **1991**, *54*, 107–136. [[CrossRef](#)]
57. Kaluthota, S.; Pearce, D.W.; Evans, L.M.; Letts, M.G.; Whitham, T.G.; Rood, S.B. Higher Photosynthetic Capacity from Higher Latitude: Foliar Characteristics and Gas Exchange of Southern, Central and Northern Populations of *Populus angustifolia*. *Tree Physiol.* **2015**, *35*, 936–948. [[CrossRef](#)]
58. Medrano, H.; Tomás, M.; Martorell, S.; Flexas, J.; Hernández, E.; Rosselló, J.; Pou, A.; Escalona, J.M.; Bota, J. From Leaf to Whole-Plant Water Use Efficiency (WUE) in Complex Canopies: Limitations of Leaf WUE as a Selection Target. *Crop J.* **2015**, *3*, 220–228. [[CrossRef](#)]
59. Franks, P.J.; Adams, M.A.; Amthor, J.S.; Barbour, M.M.; Berry, J.A.; Ellsworth, D.S.; Farquhar, G.D.; Ghannoum, O.; Lloyd, J.; McDowell, N.; et al. Sensitivity of Plants to Changing Atmospheric CO₂ Concentration: From the Geological Past to the next Century. *New Phytol.* **2013**, *197*, 1077–1094. [[CrossRef](#)] [[PubMed](#)]
60. Alía, L.A.; Lüttschwager, D.; Ewald, D. Investigation of Gas Exchange and Biometric Parameters in Isogenic Lines of Poplar Differing in Ploidy. *Silvae Genet.* **2015**, *64*, 46–59. [[CrossRef](#)]
61. Bühlmann, T.; Hiltbrunner, E.; Körner, C. *Alnus Viridis* Expansion Contributes to Excess Reactive Nitrogen Release, Reduces Biodiversity and Constrains Forest Succession in the Alps. *Alp. Bot.* **2014**, *124*, 187–191. [[CrossRef](#)]
62. Koike, T. Autumn coloring, photosynthetic performance and leaf development of deciduous broad-leaved trees in relation to forest succession. *Tree Physiol.* **1990**, *7*, 21–32. [[CrossRef](#)] [[PubMed](#)]
63. Manter, D.K.; Kerrigan, J. A/C_i Curve Analysis across a Range of Woody Plant Species: Influence of Regression Analysis Parameters and Mesophyll Conductance. *J. Exp. Bot.* **2004**, *55*, 2581–2588. [[CrossRef](#)] [[PubMed](#)]
64. Qian, T.; Elings, A.; Dieleman, J.A.; Gort, G.; Marcelis, L.F.M. Estimation of Photosynthesis Parameters for a Modified Farquhar-von Caemmerer-Berry Model Using Simultaneous Estimation Method and Nonlinear Mixed Effects Model. *Environ. Exp. Bot.* **2012**, *82*, 66–73. [[CrossRef](#)]
65. Farquhar, G.D.; Von Caemmerer, S.; Berry, J.A. Models of Photosynthesis. *Plant Physiol.* **2001**, *125*, 42–45. [[CrossRef](#)] [[PubMed](#)]
66. Miao, Z.; Xu, M.; Lathrop, R.G.; Wang, Y. Comparison of the A–C_c Curve Fitting Methods in Determining Maximum Ribulose 1·5-Bisphosphate Carboxylase/Oxygenase Carboxylation Rate, Potential Light Saturated Electron Transport Rate and Leaf Dark Respiration. *Plant Cell Environ.* **2009**, *32*, 109–122. [[CrossRef](#)] [[PubMed](#)]
67. Rostamza, M.; McNickle, G.G. A Global Database of Photosynthesis Model Parameters, and Phylogenetically Controlled Analysis of Photosynthetic Responses from Every Major Terrestrial Plant Clade. *bioRxiv* **2020**. [[CrossRef](#)]